Theoretical and experimental analyses of recording mark microstructures in signal waveform modulation optical disc*

Liu Hai-Long(刘海龙)[a)b)†], Pei Jing(裴 京)[a)], Ni Yi(倪 屹)[a)], Pan Long-Fa(潘龙法)[a)], and Tang Yi(唐 毅)[a)]

[a)] *Optical Memory National Engineering Research Center, Department of Precision Instrument, Tsinghua University, Beijing* 100084, *China*

[b)] *Measurement Technology & Instrumentation Key Lab of Hebei Province, Yanshan University, Qinhuangdao* 066004, *China*

(Received 24 November 2009; revised manuscript received 21 December 2009)

In this paper, we propose a dynamic mastering process model for signal waveform modulation (SWM) optical disc. To form the ideal microstructures and solve the problems in the SWM master manufacturing process, we use this model to simulate the three-dimensional mark profiles in the SWM read-only disc. The simulated micro-patterns of recording pits and lands are employed to optimize the writing strategy and provide a quantitative basis for manufacturing the sub-pits and sub-lands. The simulation mark profiles are compared with the experimental ones, which are produced with the optimized writing strategy parameters. Comparison results demonstrate that the simulated profiles are highly consistent with the actual ones.

Keywords: mark microstructures, SWM, mastering model, writing strategy
PACC: 4280T, 4230, 4260F

1. Introduction

Multilevel recording technology is significant for developing high density optical data storage systems. Many multilevel optical storage formats have been investigated and reported in the last ten years.[1−3] Our team also proposed two multilevel technologies on the DVD system, i.e. pit depth and width modulation (PDWM) method[4−6] and signal waveform modulation (SWM) multilevel technology.[7,8] Our multilevel disc products can be produced on a DVD manufacturing line. Hence, the advantages of PDWM and SWM are their productivity by making use of conventional DVD production technology.

Multilevel is implemented with varying recording mark microstructures in PDWM and SWM discs. In PDWM, the simultaneously varying depth and width of recording pits indicates level of the run-length. Since all the run-lengths (short T and long T, where T denotes the channel bit clock unit.) reach the same levels in PDWM, the using efficiency of longer run-lengths is lower. When the total level number of a run-length is more than 5, the readout signals of different levels of short run-lengths are overlapped and undifferentiated. The raw bit error rate (BER) evidently is improved to 10^{-3}, which cannot meet the requirements for high-definition television (HDTV) broadcasting.

To solve the problems of PDWM, in SWM disc a specific microstructure is adopted to realize multilevel. In SWM disc, the combined variation of size and position of inserted sub-pit/sub-land in an original land/pit represents level of the recording mark. To reduce the BER and improve the using efficiency of long run-lengths, the realizable level numbers of different run-lengths are variable in SWM systems. There is less or no multilevel at short run-lengths, while more levels are realized at long run-lengths.[8] With the specific microstructure, SWM disc demonstrates the following virtues: more storage capacity (land is also used to realize multilevel), lower BER (2×10^{-4}), better direct current (DC)-free control and servo performances.

Although SWM demonstrates better performance, it is very difficult for expert engineers to set appropriate writing strategy parameters to form ideal SWM multilevel recording symbols without many experiments. It is also very expensive to trail-produce

*Project supported by the National Natural Science Foundation of China (Grant Nos. 60977005 and 60677036).
†Corresponding author. E-mail: liu-hl07@mails.tsinghua.edu.cn
© 2010 Chinese Physical Society and IOP Publishing Ltd

many stampers to achieve ideal recording marks. Moreover, the variations in size and position of inserted sub-pit/sub-land can influence the signal waveform and the identifiability.

To solve the aforementioned problems, we construct an SWM master manufacturing simulation model, and use the model to establish the simulated profiles of multilevel recording symbols in SWM optical discs. The simulation results are employed to obtain the optimum writing strategy parameter for each level of every run-length. We also measure the actual microstructures of recording pits and lands in SWM with atomic force microscopy (AFM) and compare them with the simulated ones.

2. Writing strategy for SWM disc

SWM multilevel is obtained through the combined variation of size and position of inserted sub-land/sub-pit. The producing process of SWM recording marks can be explained by Fig. 1.

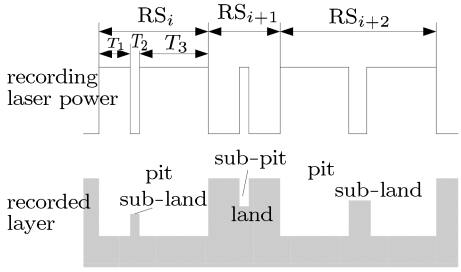


Fig. 1. Writing strategy of SWM system.

Figure 1 is the writing strategy process of SWM, which describes the relationship between timing delay of laser beam recoder (LBR) and the micro-patterns of recording marks. Run-length Series (RS) and Level Series (LS) are two output data series after error correction and modulation coding. RS$_i$ and LS$_i$ represent the length of run-length and level of pit/land, respectively.[8]

After a sub-pit or sub-land is inserted, the original SWM recording mark is split into three parts, i.e. pit-subland-pit or land-subpit-land. We define the vector $\boldsymbol{T}_{\rm P} = [T_1T_2T_3]$, whose components are corresponding to three parts of a recording mark respectively. The LS$_i$ determines the specific numbers of T_1, T_2, T_3 and their proportion, and RS$_i$ equals the summation of T_1, T_2 and T_3. That means LS$_i$ determine the position and the size of inserted sub-land or sub-pit in an original recording mark, and RS$_i$ determines the length of the original recording mark.

In SWM disc, the longer the run-length is, the more levels it will reach. In this simulated and experimental disc, the adopted modulation code is a bi-modulation code with a code rate of 7/8.[8] There is no multilevel at 2–3T, and the level numbers of 4-11T are 2, 3, 4, 4, 5, 5, 7 and 7, respectively. Table 1 gives the relationship between the combined variation of size and position of inserted sub-pit/sub-land and level of a run-length. For example, if a large sub-land/sub-pit is inserted into the middle of the original 5T pit/land, the recording mark is called level 2 of 5T pit/land. Level 1of 5T pit/land means inserting a small sub-pit/sub-land into the middle of the original 5T recording land/pit. Oppositely, if there is no inserted sub-mark, it is defined as level 0 of 5T pit/land.

Table 1. Combined variation of size and position of sub-symbols with different levels.

level of a run-length	level 0	level 1	level 2	level 3	level 4	level 5	level 6
size of sub-pit/sub-land	no	large	large	large	small	small	small
position of sub-pit/sub-land	no	middle	left	right	middle	left	right

The concepts of large small, middle, left and right in Table 1 are qualitative parameters and cannot be used directly to form the profiles of SWM recording marks. These concepts are represented by quantitative parameter $\boldsymbol{T}_{\rm P}$. Thus, the appropriate $\boldsymbol{T}_{\rm P}$ for each level of every run-length must be elaborately designed with simulation results to form appropriate microstructure.

To select the appropriate $\boldsymbol{T}_{\rm P}$, we build a dynamic simulator for SWM disc. The simulator mainly comprises the intensity profile of beam spot, exposure process model and developing photoresist models.

3. Mastering simulator

Richards and Wolf,[9] and Boivin and Wolf[10] gave the model of the focused intensity distribution of an incident laser beam coming through a focusing objective lens. We use cylindrical coordinate (ρ, φ, z) to describe

the electric field near the focal point. The intensity profile of the beam spot is determined by the light electric field near the focal point. Kathleen and Thomas[11] calculated the cylindrical-vector fields and summarized as the following formulas:

$$I = |e|^2, \tag{1}$$

$$e_\rho^{\mathrm{s}} = A_{\mathrm{s}} \int_0^\alpha \cos^{1/2}\theta \sin(2\theta) l_0(\theta) J_1(k\rho_{\mathrm{s}} \sin\theta) \exp(\mathrm{i}\, kz\cos\theta)\mathrm{d}\theta,$$

$$e_\phi^{\mathrm{s}} = 2A_{\mathrm{s}} \int_0^\alpha \cos^{1/2}\theta \sin\theta \cdot l_0(\theta) J_1(k\rho_{\mathrm{s}} \sin\theta) \exp(\mathrm{i}\, kz\cos\theta)\mathrm{d}\theta,$$

$$e_z^{\mathrm{s}} = 2iA_{\mathrm{s}} \int_0^\alpha \cos^{1/2}\theta \sin^2\theta \cdot l_0(\theta) J_0(k\rho_{\mathrm{s}} \sin\theta) \exp(\mathrm{i}\, kz\cos\theta)\mathrm{d}\theta,$$

where, e_ρ^{s}, e_ϕ^{s} and e_z^{s} are respectively the radial, the azimuthal, and the longitudinal components of the electric field vector near focus in the cylindrical coordinates; function $J_n(k\rho_{\mathrm{s}} \sin\theta)$ denotes a Bessel function of the first kind of order n; $k = 2\pi/\lambda$; $\alpha = \sin^{-1}(NA/n)$;

$$l_0(\theta) = \exp\left[-\beta_0^2\left(\frac{\sin\theta}{\sin\alpha}\right)^2\right] J_1\left(2\beta_0 \frac{\sin\theta}{\sin\alpha}\right)$$

with parameter β_0 being the ratio of pupil radius to beam waist.

Dill *et al.*[12] and Pasman *et al.*[13] researched the integrated circuit (IC)-lithography model, which was adopted to describe the exposure model in disc mastering. Considering the special characteristic of disc mastering, Song *et al.*[14] and Yuan *et al.*[15] predigested the model and described it as

$$M(x, y, t) = M(x, y)\mathrm{e}^{-CE(x,y)}, \tag{2}$$

where M is the photo active compound concentration relative to the initial concentration, E is the exposure dose and can be calculated from

$$E(x, y, t) = \int_0^t I(x, y, \tau)\mathrm{d}\tau. \tag{3}$$

Kim *et al.*,[16] Trefonas and Daniels,[17] and Hirai *et al.*[18] all separately developed the model of IC-lithography. Of all the three models, the Trefonas *et al*'s model is the simplest, and the number of parameters needed to be demarcated is the smallest. We adopt it as the simulation model, which is expressed as

$$R = R_0(1 - M)^q, \tag{4}$$

where R_0 is the development rate of fully exposed photoresist and q is the photoresist contrast. The main parameters used in simulation and disc mastering are shown in Table 2.

Table 2. Parameters used in simulation and master manufacturing.

parameters	sign	value
the maximum developing rate	R_0	12 nm/s
developing contrast	q	2.3
developing time	t_{d}	12 s
photoresist constant	C	2.6 mm^2/(mJ·s)
recording speed	v	3.52 m/s
focus spot intensity	I_0	16.4 mW/μm^2

4. Simulated and experimental results

The simulation model is employed to generate the microstructure of each level of every run-length and optimize the writing strategy parameter T_{P}. Based on simulated results, the optimum T_{P} of each level of every run-length is designed and confirmed. Table 3 gives the optimum T_{P} of levels of $5T$, $8T$ and $10T$.

Table 3. Optimum T_{P}'s of $5T$, $8T$ and $10T$.

	T_{P} of $5T$	T_{P} of $8T$	T_{P} of $10T$
level 0	[22.5 0 22.5]/9	[36 0 36]/9	[45 0 45]/9
level 1	[19 7 19]/9	[29.5 13 29.5]/9	[38.5 13 38.5]/9
level 2	[16.5 12 16.5]/9	[24 13 35]/9	[31 13 46]/9
level 3		[35 13 24]/9	[46 13 31]/9
level 4		[32.5 7 32.5]/9	[41 8 41]/9
level 5			[30 9 51]/9
level 6			[51 9 30]/9

Figure 2 shows some parts of the simulation results in a recording track with optimum $T_{\rm P}$, and it illustrates the simulation profiles of level 0 of $3T$ pit, level 2 of $9T$ land, level 4 of $8T$ pit, and level 4 of $8T$ land (partly). The sizes of 2 sub-pits in this figure are different from each other, which is used for explaining the levels of run-lengths.

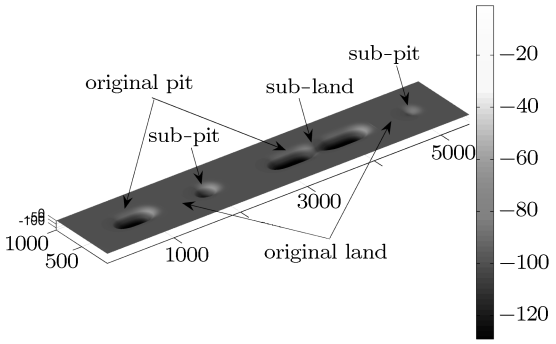
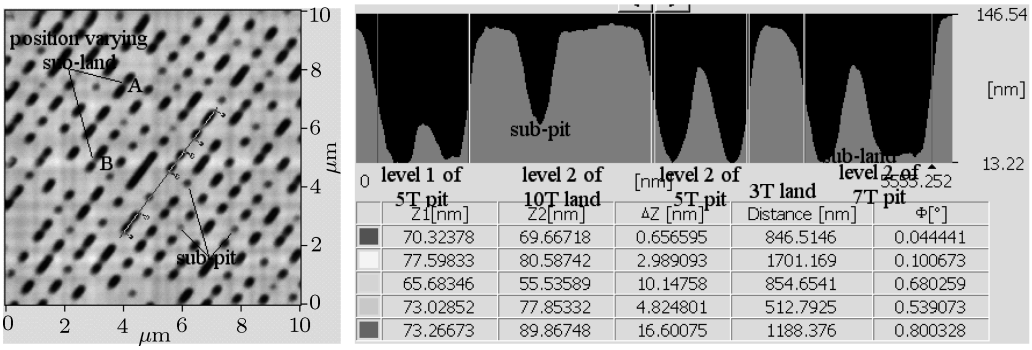


Fig. 2. Simulation of the recording symbols of a track.

Figure 3 shows the AFM image of experiment SWM disc, which is produced with optimum $T_{\rm P}$. In Fig. 3(a), we can clearly see the variations in size and position of sub-pit/sub-land. Figure 3(b) gives the detailed microstructures of a track. The run-length is judged by the distances between four pairs of lines. The length of $1T$ in the experimental SWM disc is designed to be 170 nm. The level information of the recording marks is determined by the size and the position of inserted sub-pit/sub-land. According to Table 1 and the measured distances, the recording marks are in turn level 3 of $6T$ land, level 1 of $4T$ pit, level 0 of $2T$ land, and level 1 of $5T$ pit. Comparing Fig. 2 with Fig. 3 leads to a conclusion that $T_{\rm P}$ obtained from the simulation results satisfies the high precision requirement of SWM disc.

We take $8T$ as an example to describe the relationship between $T_{\rm P}$ and simulation micro-patterns of the SWM recording symbols. According to Table 3, [36 0 36]/9, [29.5 13 29.5]/9, [24 13 35]/9, [35 13 24]/9, [32.5 7 32.5]/9 are respectively set as the values of $T_{\rm P}$ of levels 0–4 of $8T$. The corresponding simulation profiles of $8T$ recording pits are shown in Fig. 4. The accuracy of simulation reaches up to 19 nm ($T/9$). Figures 4(a)– 4(e) show the simulated microstructures of $8T$ pits with levels 0–4. Figures 4(f)–4(j) exhibit the contour maps of $8T$ pits with levels 0–4. Comparing Fig. 4(b) with Fig. 4(e), we can see that the inserted sub-lands are both in the middle of $8T$ pits. However, the sizes of inserted sub-lands are changed, which is used for denoting levels 1 and 4 of $8T$ pits. Figures 4(b)–4(d) show the position variations in inserted large sub-land, which are used to differentiate levels 1, 2 and 3 of $8T$ pits. There is no inserted sub-land in $8T$ pits in Fig. 4(a). Hence, Fig. 4(a) represents the microstructure of level 0 of $8T$ pit.



(a) (b)

Fig. 3. AFM image of SWM disc.

To verify the correctness of simulation results, we use the same parameters to produce the SWM disc. The microstructures of $8T$ recording pits are scanned and analysed with AFM and SPI3800N analysis software. Figure 5 shows the actual profiles of $8T$ pits with levels 1–4. Figures 5(a) and 5(d) indicate the size variations of sub-lands, while Figs. 4(a)–4(c) illuminate the position variations of inserted sub-lands.

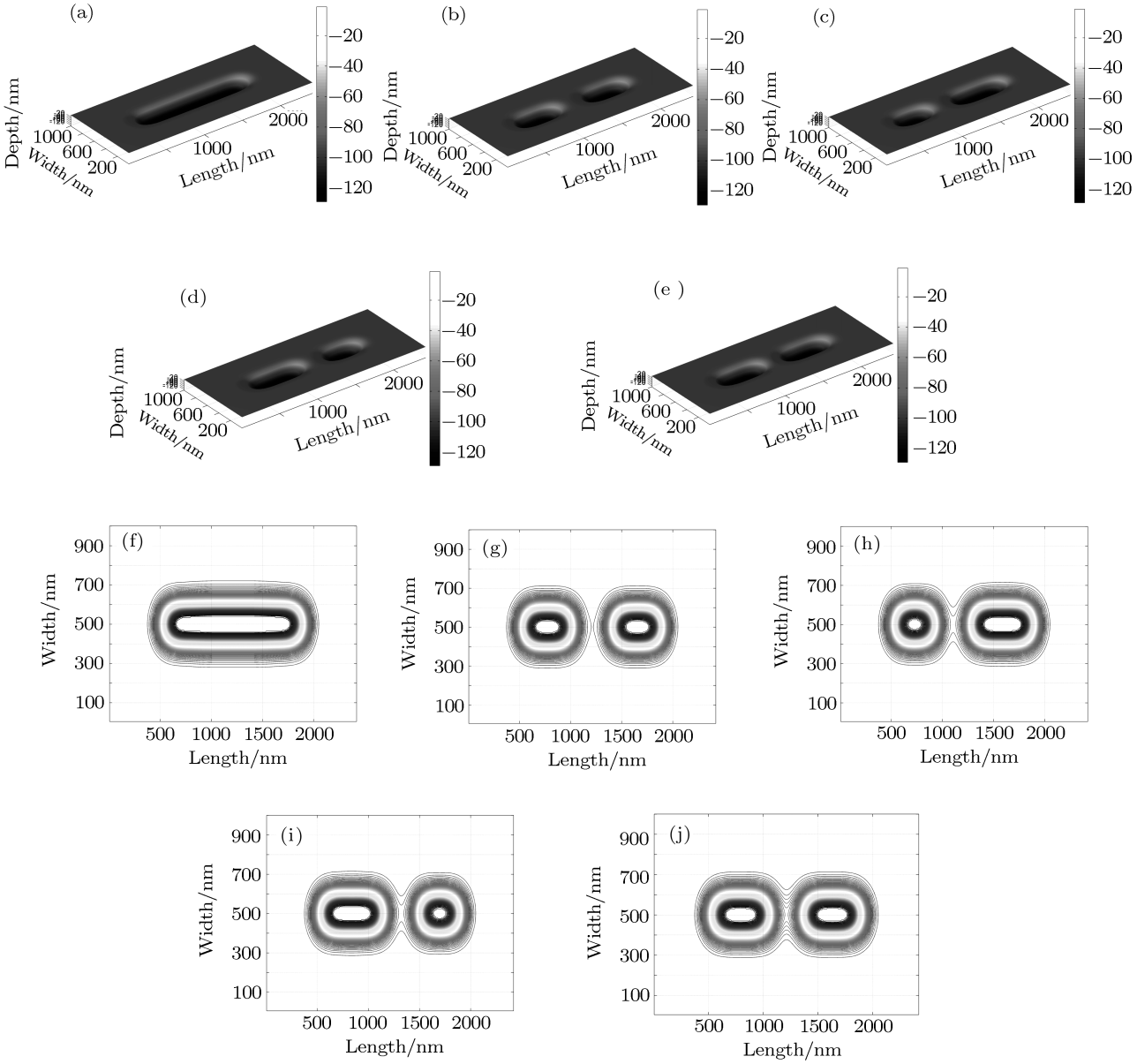


Fig. 4. Simulated microstructures ((a)–(e)) and contour maps ((f)–(j)) for 8T pits with levels 0–4.

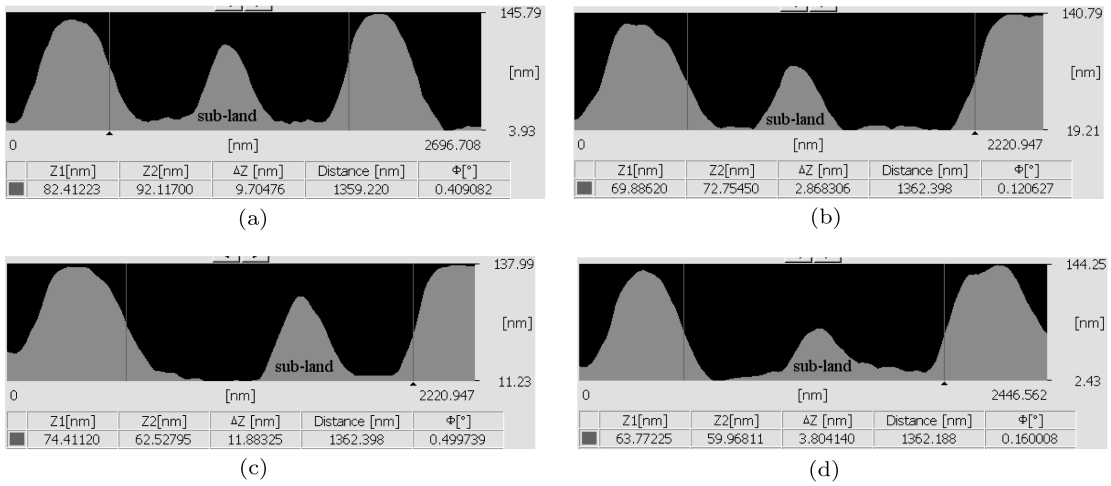


Fig. 5. Microstructures of 8T pits with levels 1 (a), 2 (b), 3 (c), 4 (d) of 8T pit.

Comparing Fig. 4 with Fig. 5, we can see that the simulated structures are consistent with the actual ones. The simulation results reveal the actual profiles of different levels of $8T$ recording pits with an accuracy of 19nm. Hence, the optimum writing strategy parameter $T_{\rm P}$ based on simulation results is suited to form ideal microstructures of SWM recording marks. It is time-saving to manufacture the SWM disc designed with the simulation results. It is also helpful to reduce hazardous wastes. Moreover, we can change the vector $T_{\rm P}$ to verify the realizable maximum level number of a run-length and provide some theoretical instructions for SWM disc mastering.

5. Conclusions

In multilevel optical recording systems, the microstructures of recording symbols can be used for recognizing levels of a run-length. In this paper, we use the master producing model to simulate the profiles of multilevel recording symbols in an SWM system. The experimental results reveal that the simulation micro-patterns accord well with the actual ones. The simulation accuracy of recording mark microstructures reaches up to 19 nm.

The SWM disc has advantages of higher capacity, lower BER and better servo performance. Therefore, the SWM is a promising optical recording technology and can be an option of HDTV times. Our work in this paper is used for optimizing the writing strategy parameter and fabricating ideal SWM disc.

References

[1] Nakajima J, Terashima S and Ohta K 2001 *Jpn. J. Appl. Phys.* **40** 1846

[2] Kobayashi S, Yamatsu H and Takemoto Y 2001 *Jpn. J. Appl. Phys.* **40** 1704

[3] Nishida T Shintani T and Maeda T 2005 *Jpn. J. Appl. Phys.* **44** 193

[4] Zhang Q C, Ni Y, Xu D Y, Hu H, Song J and Hu H 2006 *Jpn. J. Appl. Phys.* **45** 4097

[5] Song J, Xu D Y, Qi G S, Hu H, Zhang Q C and Xiong J P 2006 *Chin. Phys.* **15** 1788

[6] Hu H, Xiong J P, Xu D Y, Qi G S, Xiao J X and Hu H 2007 *Acta Phys. Sin.* **56** 208 (in Chinese)

[7] Tang Y, Pei J, Ni Y, Pan L F, Hu H and Zhang B Q 2008 *Opt. Express* **16** 6156

[8] Liu H L, Pei J, Pan L F, Tang Y and Liu X W 2009 *Electron. Lett.* **45** 906

[9] Richards B and Wolf E 1959 *Proc. R. Soc.* Ser. A **253** 358

[10] Boivin A and Wolf E 1965 *Phys. Rev.* **138** 1561

[11] Kathleen Y and Thomas B 2000 *Opt. Express* **7** 77

[12] Dill F, Neureurther A and Tuttle J 1975 *IEEE Trans. Electron. Devices* **22** 456

[13] Pasman J, Put P and Kraakaman P 1992 *Proc. SPIE* **1663** 336

[14] Song J, Ni Y, Xu D Y, Pan L F, Zhang Q C and Hu H 2006 *Opt. Express* **14** 1199

[15] Yuan H B, Xu D Y, Zhang Q C and Song J 2007 *Opt. Express* **15** 4176

[16] Kim D, Oldham W and Neureuther A 1984 *IEEE Trans. Electron Devices* **31** 1730

[17] Trefonas P and Daniels B 1987 *Proc. SPIE* **771** 194

[18] Hirai Y, Sasago M, Endo M, Tsuji D and Mano Y 1987 *IEEE Trans. Computer-Aided Design* **6** 403